ELSEVIER

Polymer 43 (2002) 4207–4216

polymer

www.elsevier.com/locate/polymer

Nanopatterned surfaces obtained with semicrystalline ABC triblock copolymers

V. Balsamo[a,*], S. Collins[b], I.W. Hamley[b]

[a]*Grupo de Polímeros USB, Departamento de Ciencia de los Materiales, Universidad Simón Bolívar, Aptdo. 89000, Caracas 1080A, Venezuela*
[b]*Department of Chemistry, University of Leeds, Leeds LS2 9JT, UK*

Received 16 August 2001; received in revised form 20 February 2002; accepted 6 March 2002

Abstract

The surface patterns resulting from fast crystallization of as-cast and annealed thin films (ca. 100 nm) of two polystyrene-*b*-polybutadiene-*b*-poly(ε-caprolactone) ABC triblock copolymers is investigated through atomic force microscopy (AFM). Two different substrates are used: silicon and mica. The behaviour is compared with the bulk morphology obtained through transmission electron microscopy (TEM). AFM images of the as-cast films revealed surfaces with lamellar patterns. Based on the observation of T-shaped grain boundaries between lamellae, and on a comparison of the microdomain dimensions obtained by TEM and AFM, the surface pattern is rationalized as being formed by amorphous and crystalline polycaprolactone (PCL), with the PCL/PB block copolymer interfaces located parallel to the susbstrate. The formation of islands and holes in annealed films with a lamellar 'floor', depending on the conmensurability between film thickness and long period, is also observed, indicating a parallel orientation of the block copolymer lamellae. © 2002 Published by Elsevier Science Ltd.

Keywords: ABC triblock copolymers; Polycaprolactone based semicrystalline copolymers; Atomic force microscopy

1. Introduction

Crystallization in polymers continues to attract attention, despite several decades of research, because important issues such as the mechanism of crystallization are still not understood. Semicrystalline diblock copolymers offer model systems where the effect of a tethered amorphous block on the crystal stem orientation and crystallization mechanism can be investigated, and a number of recent studies have focused on these materials [1–5].

The morphology upon crystallization in semicrystalline diblock copolymers is greatly influenced by the extent of segregation of the copolymer or the presence of glassy microdomains. Crystallization can overwhelm the micro-phase-separated structure formed in a weakly segregated diblock melt [6–8]. However, glassy domains lead to 'nanoscale confinement' of crystal lamellae, and hence constrain the crystal stem orientation [9–12]. If the block copolymer is strongly segregated, crystallization can be guided by [8] or occur within [12,13] the microdomains in the pre-existing melt morphology. A review of the subject has recently appeared [14].

The experimental and theoretical work on block copolymers deals mainly with the bulk morphology, and there is only a limited amount of information on the structure and orientation of microdomains in thin films. Crystallization in thin films of hPB-*b*-PEO diblocks has recently been investigated by Reiter et al. [15,16]. For a diblock containing 45% PEO they observed, using atomic force microscopy (AFM), lamellae oriented parallel lamellae in the melt but perpendicular to the substrate upon crystallization at a large undercooling [16]. Within this arrangement, the lamellar surface is proposed to be formed by alternating PEO and PB lamellae. This was ascribed to a kinetically trapped state of chain-folded PEO crystals. The perpendicular lamellae could be preferentially aligned over several micrometers when crystallization occurred close to a three-phase contact line. However, ultimately the morphology evolved into the equilibrium parallel one, which was also observed for three other diblocks with a higher PEO content [16]. Films of these copolymers were characterized by smooth islands and holes at the surface due to an incommensurability between the film thickness and an integral number of lamellae. The island and hole structure was retained upon crystallization, although craters and cracks appeared in the lamellae. Within craters, terracing of lamellar steps was observed,

* Corresponding author.
E-mail addresses: vbalsamo@usb.ve (V. Balsamo), s.collins@chem.leeds.ac.uk (S. Collins), ianh@chem.leeds.ac.uk (I.W. Hamley).

0032-3861/02/$ - see front matter © 2002 Published by Elsevier Science Ltd.
PII: S0032-3861(02)00185-4

from which the lamellar thickness could be extracted. Terracing of crystal lamellae oriented parallel to the substrate was also reported for a PEO-*b*-PBO diblock and a PEO-*b*-PBO-*b*-PEO (PBO = poly(oxybutylene)) triblock, probed via AFM [17]. In this work a comparison of the lamellar thickness was also made with the domain spacing obtained from small-angle X-ray scattering (SAXS) and a model of tilted chains was proposed (fully extended for the diblock, once folded for the triblock). However, this is not in agreement with recent simultaneous SAXS/WAXS (wide angle X-ray scattering) results that indicate PEO chains oriented perpendicular to lamellae in a PEO-*b*-PBO diblock [18].

Thus, most studies to date have been limited to AB diblock and ABA triblock copolymers. Recently, the interplay between crystallization and microphase separation in hydrogenated and non-hydrogenated ABC triblock copolymers of polystyrene, polybutadiene and polycaprolactone (PCL) in the bulk has been examined [19–22]. It was found that the crystallizable blocks have a significant influence on the mesophase structure in spite of the presence of a glassy polystyrene block. The microdomains do not show the same degree of long-range order as in amorphous ABC triblock copolymers. Moreover, a change of the crystallization conditions can induce a morphological transition, for example, from a lamellar–lamellar (ll) to a lamellar–cylindrical (lc) morphology [22]. These results together with the previously demonstrated formation of well-defined spherulites give strong evidence of a perpendicular orientation of the crystalline PCL (cPCL) chain stems with respect to the block copolymer interfaces. On the other hand, Jackson and co-workers [23,24] have reported that the formation of spherulites in a copolymer with 50% PCL depends on sample thickness.

To our knowledge, studies on the surface morphology of thin films of ABC triblock copolymers have been limited to amorphous ones [25–27]. These works have shown that it is possible to obtain perpendicular arranged lamellae, as is also the case for diblocks if the film is thin enough or if it is confined between two walls. The formation of such patterned surfaces could be very interesting for potential applications.

In this work we explore the surface morphology of thin films (thickness ca. 100 nm) of two semicrystalline ABC polystyrene-*b*-polybutadiene-*b*-PCL triblock copolymers, which form ll- and lc-morphologies in the bulk. We show that the commensurability between film thickness and long period is a determining factor in obtaining a lamellar nanopatterned surface. Models that explain these observations with the simultaneous formation of islands and holes are presented.

2. Experimental section

2.1. Materials

Two poly(styrene-*b*-butadiene-*b*-ε-caprolactone) ABC triblock copolymers were synthesized via anionic polymerization [28]. The molecular characteristics of the materials are summarized in Table 1.

Table 1
Molecular characteristics of the triblock copolymers used in this study

Copolymer[a]	$M_n \times 10^{-3}$ (g/mol)[b]	M_w/M_n	1,2 PB units (wt%)
$S_{27}B_{15}C_{58}$	219	1.30	10
$S_{35}B_{15}C_{50}$	150	1.22	11

[a] The subscripts represent the weight percent of each component.
[b] Determined from ^{1}H NMR using $M_{n\,PS}$ obtained from GPC curves, calibrated with PS standards.

2.2. Transmission electron microscopy

Films of ~1 mm thick were slowly cast from 5 wt% toluene solutions and dried under vacuum for one day at room temperature. They were then annealed at 150 °C for 15 h under vacuum, cooled down to 40 °C, held at that temperature for 3 h and quenched to room temperature. Ultrathin sections (~40 nm thick) were obtained at −120 °C using a Leica Ultracut UCT Ultramicrotome equipped with a diamond knife. The ultrathin sections were subsequently stained using osmium tetroxide under vacuum at room temperature. Transmission electron microscopy (TEM) was performed in the bright field mode on a Jeol JEM 1220, operating at 100 kV.

2.3. Atomic force microscopy

Thin films (approximate thickness 100 nm) were obtained through spin coating at 2500 rpm for $S_{35}B_{15}C_{50}$ and 3000 rpm for $S_{27}B_{15}C_{58}$ from 2 wt% toluene solutions on silicon wafers, without previous treatment of the substrate surface. Some of the films were used as cast after drying in a vacuum oven at room temperature; other samples were annealed at 150 °C for various times (5, 10 and 15 h). After annealing, the films were quenched to room temperature. The sample surfaces were investigated using a Digital Instruments multimode AFM with a Nanoscope IIIa controller. Topographic and phase images were recorded simultaneously using tapping mode with Si tips. Film thicknesses were determined by AFM scans using the following procedure: After scanning the sample in tapping mode, the sample (~1 μm width) was scanned again in contact mode (but using the same tapping tip). The tapping tip is too forceful for contact mode AFM and so has the effect of scraping a hole in the film. The AFM was converted back to tapping mode and the sample was scanned again, but over a larger area, typically 4 μm width (Fig. 1(a)). Cross-section analysis was then performed to measure the difference in height between the inside and outside of the hole (Fig. 1(b)). The height and distance differences between markers on the far left and far right side of the cross-section was used to determine the (small) slope of the surface. This was then used to correct for the difference in height between the markers each side of an edge of the hole. A number of measurements

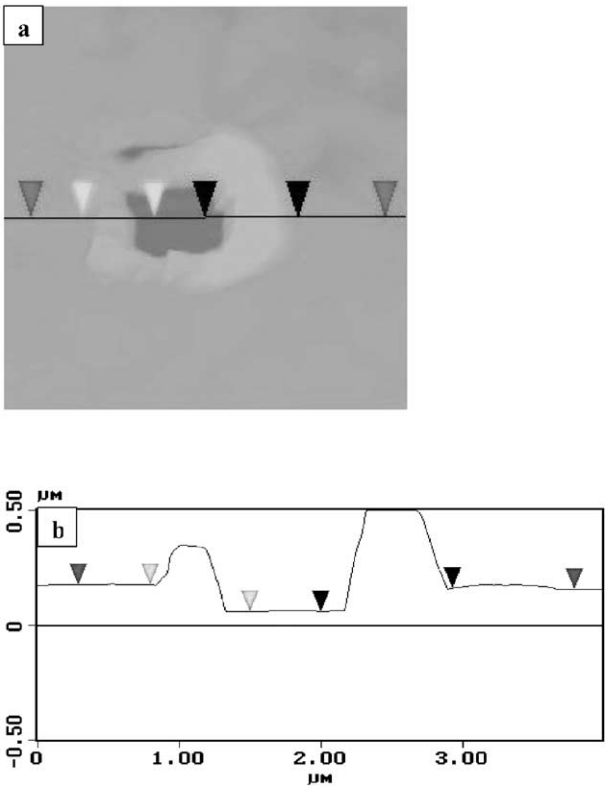

Fig. 1. (a) Topographic AFM image of the surface obtained for $S_{27}B_{15}C_{58}$ (spin coated on silicon and annealed at 150 °C for 15 h) (Fig. 9) after scrapping a hole. (b) Cross-sectional line scan.

(2–10) around the edge of the hole were made and the results were averaged. A blank test was performed on a silicon wafer (with no polymer film) to ensure that the AFM tip was not scraping its surface. The AFM calibration was checked using a TGZ01 grid (from NT-MDT) and found to be within 5% (i.e. less than the manufacturing tolerance of the grid).

2.4. Differential scanning calorimetry (DSC)

PCL-block melting points and degree of crystallinity were determined using a Perkin–Elmer DSC Pyris 1 at a heating rate of 10 °C/min under a helium atmosphere. A value of 163 J/cm^3 was used for the melting enthalpy of 100% cPCL [29].

3. Results and discussion

We start our discussion by considering the bulk morphology obtained for the $S_{27}B_{15}C_{58}$ triblock copolymer by TEM, because it will be used as a reference for the forthcoming discussion of the AFM results. This triblock exhibits, under the conditions mentioned in Section 2, a ll-morphology in the bulk as can be observed in Fig. 2. Using OsO_4 as staining agent, the polybutadiene block appears as dark lamellae of thickness L_{PB} between grey polystyrene (L_{PS}) and bright

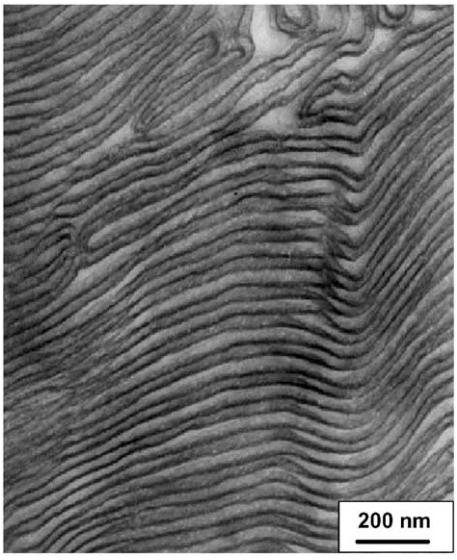

Fig. 2. Transmission electron micrograph of $S_{27}B_{15}C_{58}$.

PCL (L_{PCL}) lamellae. A schematic description of this morphology and the bulk long period is shown in Fig. 3.

As mentioned in Section 2, for the AFM studies topographic (height mode) and viscoelastic (phase mode) data were recorded simultaneously. It should be noted that semicrystalline polymers are well suited for the use of the 'phase mode' as the difference in viscoelastic properties between crystalline and amorphous regions is large. This allows an imaging mode, which is complementary to the more widely used height imaging mode [16]. Therefore, in the specific case of the triblock copolymers under study, we expect phase contrast not only between the different chemical components like PB/PS or PB/PCL, but also between the amorphous PCL (aPCL) and cPCL regions. The latter is possible due to the degree of crystallinity of the PCL block of ~60% determined through DSC measurements from samples treated similarly to the samples used for AFM studies.

Fig. 4 shows a lamellar patterned surface for the as-cast $S_{27}B_{15}C_{58}$ sample (without annealing). This pattern can only be clearly appreciated in the phase image. Lamellae oriented perpendicular to the surface can be identified, the lamellae exhibiting some curvature. Two regions can be

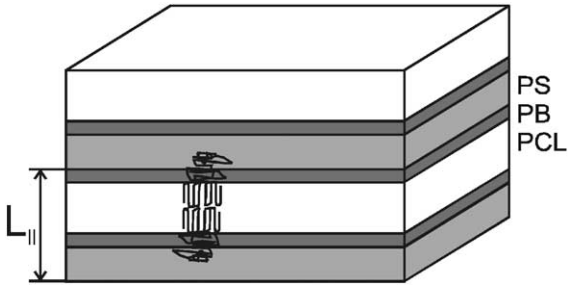

Fig. 3. Schematic description of the ll-morphology. For $S_{27}B_{15}C_{58}$ $L_{ll} = 93 \pm 2$ nm, $L_{PS} = 27 \pm 3$ nm, $L_{PB} = 15 \pm 2$ nm, $L_{PCL} = 30 \pm 3$ nm.

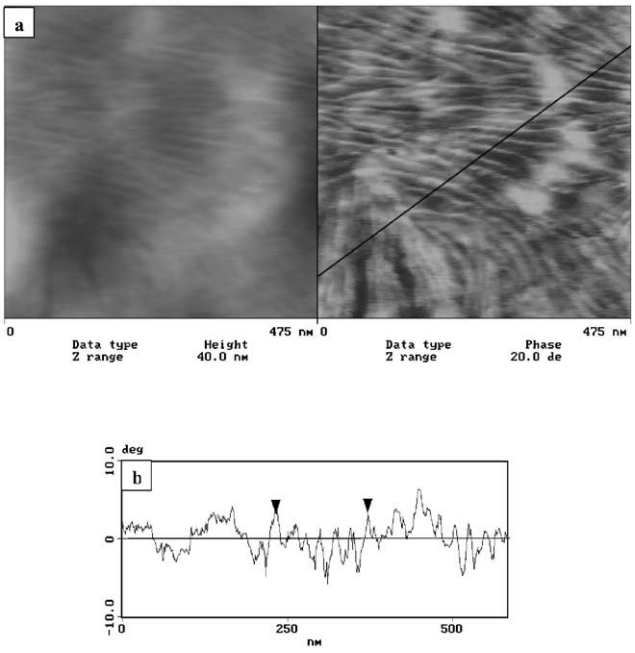

Fig. 4. (a) Topographic (left) and phase (right) AFM images of the as-cast $S_{27}B_{15}C_{58}$ sample on silicon. (b) Cross-sectional line scan of the upper part of the phase image.

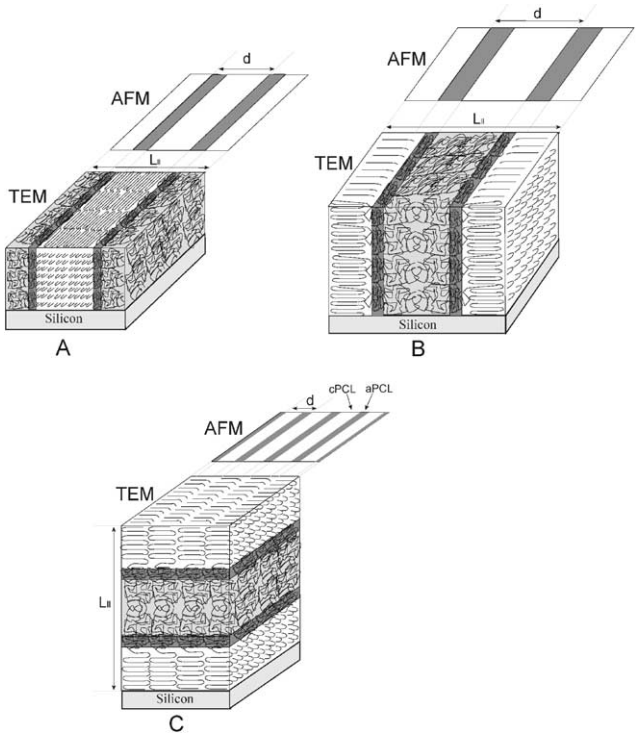

Fig. 5. Schematic representations of the possible ordering of $S_{27}B_{15}C_{58}$ on a substrate. AFM projections show the contrast that would be obtained in the phase images of the surfaces. Three-dimensional structures show the contrast that is obtained in the bulk after OsO_4 staining (PS: grey, PB: black and PCL: white).

distinguished: in the bottom part of the figure the characteristic distance appears to be larger. An accompanying line scan for the upper part of the image defines an average peak distance of $d = 24 \pm 2$ nm corresponding to the sequence of 'hard' and 'soft' regions indicated by 'lines' in the image.

To understand the origin of this pattern, the different ways that such a copolymer can self-assemble on a substrate must be considered. Taking as a reference the bulk morphology, a schematic representation of three possible models is shown in Fig. 5. Based on the viscoelastic properties of the components we assumed the complex case in which there is no phase contrast between PS and cPCL or between PB and aPCL. Models A and B can be discarded because the average lateral period (L_p) does not correspond at all to the bulk long period dimensions (L_{ll}), which corresponds to the sequence ABCB… In this case the thickness of two bright domains (PS and cPCL) and two dark domains (each one composed of PB and aPCL) should be taken for the calculation of the lateral period (L_p) in the AFM image (Fig. 5). A value of $L_p = 48$ nm is obtained, which is quite far from the bulk long period (L_{ll}) of 93 ± 2 nm determined through TEM. Consequently, we have adopted model C. According to the depth measurements performed through AFM, this film has a thickness (h) of 122 ± 4 nm. This value indicates the presence of more than one layer of ABC molecules arranged on the substrate. Although we have not investigated directly how the film is organized beneath the surface, it could be speculated, based on L_{ll} and h that the film is formed by three layers of ABC molecules, with slightly tilted lamellae. In fact, the apparent larger long period observed in some regions (bottom) of the phase image in Fig. 4(a), could be explained by such a slight tilting of the lamellae with respect to the substrate. Such tilting of the lamellae on a substrate has been previously reported for oxyethylene/oxybutylene block copolymers [17].

The same morphology can be observed in Fig. 6 when the substrate was changed to mica. Nevertheless, we present this figure because a better resolution of the phases could be obtained, even making it possible to distinguish an isolated lamella (see arrow) in the magnified image of Fig. 6(b). The observation of T-shaped grain boundaries [30] between lamellae is only likely within model C, since the lamellae are oriented perpendicular to the substrate in this model. Sharp changes in grain orientation would be prohibited if block copolymer interfaces were perpendicular to the surface as in models A or B. It is important to note this arrangement is different from that proposed by Reiter et al. [15,16] in hydrogenated polybutadiene-*b*-poly(ethylene oxide) diblock copolymers, because when they were able to distinguish a surface lamellar pattern, it was attributed to a sequence of PEO and hPB lamellae, with a perpendicular orientation of the block copolymer interfaces with respect to the substrate. On the other hand, under conditions in which a parallel orientation of the diblock copolymer interfaces was proposed, they did not distinguish a lamellar pattern on the surface. In our triblock copolymers we propose a parallel orientation of the block copolymer interfaces with respect to

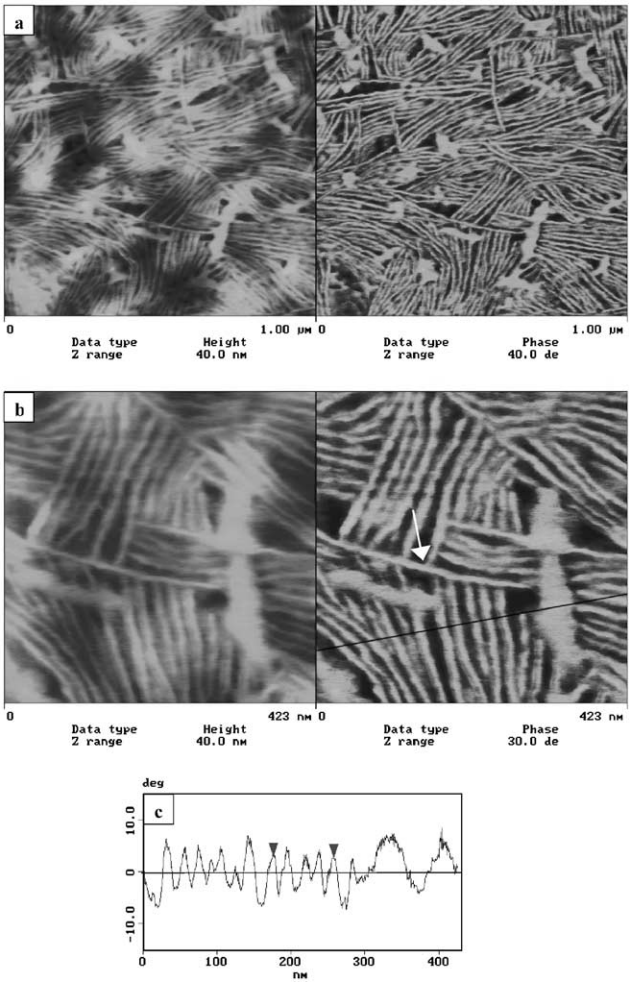

Fig. 6. (a) Topographic (left) and phase (right) AFM images of the surface obtained for $S_{27}B_{15}C_{58}$ spin coated on mica. (b) Magnification of (a). (c) Cross-sectional line scan.

the substrate together with a surface lamellar pattern, which is caused by sequences of aPCL and cPCL.

The cross-sectional analysis of this image (Fig. 6(c)) showed an average peak distance of $d = 20 \pm 2$ nm, in agreement with the results obtained on silicon. Due to the high resolution obtained in this case, a more accurate measurement of the crystalline lamella thickness could be performed, leading to a value of ~11 nm. A rough calculus of the theoretical lamellar thickness was performed using the Thompson–Gibbs equation [31]

$$l = 2\sigma_e T_m^0 / \left(\Delta H_m^0 \left(T_m^0 - T_m\right)\right) \quad (1)$$

where T_m^0 is the equilibrium melting point obtained for the PCL-block of this copolymer (65.3 °C), T_m is the dynamic melting point measured by DSC after a similar thermal treatment (57 °C), σ_e is the fold surface energy, estimated to be 4.469×10^{-6} J/cm^2 [32], ΔH_m^0 is the melting enthalpy for a 100% cPCL homopolymer (163 J/cm^3) [29]. The calculated value of 22 nm is twice that of the experimental one. It is known that the Thompson–Gibbs equation can overestimate the lamellar thickness due to the higher melting temperature (T_m) of annealed crystals when the original ones are unstable. Such a situation could have arisen here from the fast solvent evaporation process used. In fact, this process is probably responsible for the rough surfaces obtained in the as-cast samples.

It has previously been shown that this material is able to form spherulites under controlled crystallization conditions [22]. In order to investigate this aspect, the spin-coated sample on mica was directly observed under polarizing light in the optical microscope. No spherulites were observed (down to 4 μm). This is probably due to the fast evaporation of the solvent. However, in the AFM images the observation of some curving of the lamellae (as well as the rough surface) could be a sign of incipient three-dimensional ordering.

The crystalline stems are depicted in model C of Fig. 5 parallel to the lamellar surfaces, in contrast to the proposal of Balsamo et al. [22], due to the fast crystallization process. Under such conditions, the chain segments probably do not have enough time to arrange themselves perpendicular to the interface. It has been shown that the orientation of the crystalline stems with respect to the interfaces depends on the crystallization pathway and glass transition of the amorphous components. In general, a restricted mobility of the crystalline chains, caused by the presence of a glassy amorphous component, by the crystallization conditions (quenching) or by strong segregation of the blocks, leads to a parallel orientation of the crystalline stems due to a confinement effect [8–12,14]. In the specific case of the $S_{27}B_{15}C_{58}$ triblock copolymer, there are some indications that the chain segments could be aligned parallel or perpendicular to the interfaces depending on the annealing time at high temperatures in the melt [33].

It should be mentioned that some discrepancies between the dimensions taken from the previous AFM and TEM images could arise from the different crystallization conditions. TEM images were obtained from samples crystallized from the melt, whereas AFM images from samples which rapidly crystallized from solution in the spin coating process. Therefore, we prepared samples for AFM experiments, which were annealed at 150 °C. However, it should be taken into account that crystallization can also be affected by the thickness of the samples when comparing TEM with AFM results.

When the thin films deposited on silicon wafers were annealed at 150 °C for 5 h, an apparent change of the surface morphology occurred, as can be observed in Fig. 7, which was obtained following a quench to room temperature. Featureless islands are observed randomly located throughout the surface. The cross-sectional analysis reveals an average height of the islands (δh) of about 23 ± 6 nm. The surface of the underlying layer again exhibits a perpendicular lamellar structure.

In the ordered state, thin films of block copolymers form

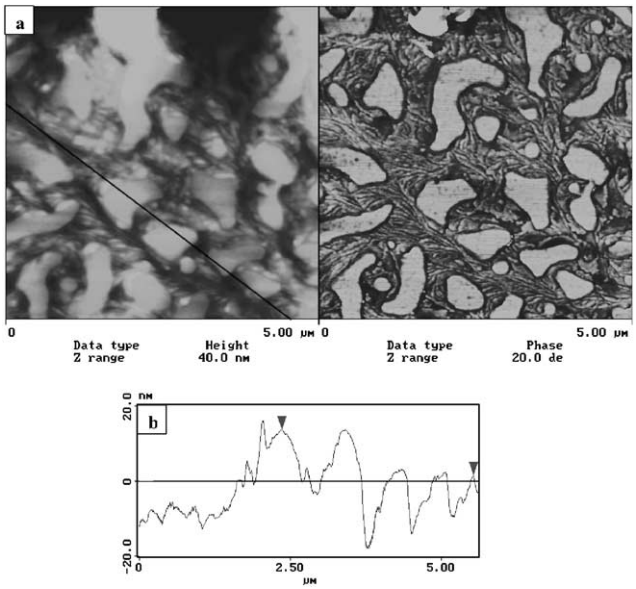

Fig. 7. (a) Topographic (left) and phase (right) AFM images of $S_{27}B_{15}C_{58}$ spin coated on silicon and annealed at 150 °C for 5 h. (b) Cross-sectional line scan.

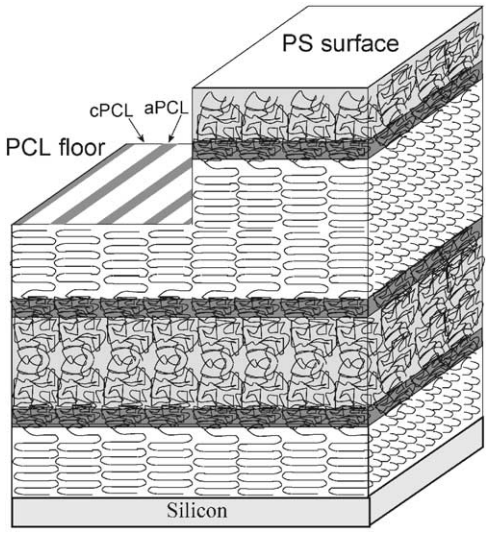

Fig. 8. Schematic representation of islands on a PCL floor for the $S_{27}B_{15}C_{58}$ copolymer.

islands or holes (height or depth δh), when the film thickness (h) is incommensurate with the bulk long period, L_{ll}. The islands and holes are, therefore, created from excess material not used to form a complete ordered layer [34]. In our case, the islands could be the result of such excess material. Previous studies on amorphous AB and ABA block copolymers [34–38] have shown that in the usual case of asymmetric wetting the total film thickness is defined by

$$h = (n + 1/2)L + \delta h \quad (2)$$

where n is an integer, L the bulk long period and the magnitude of δh defines the features of the surface. Discrete holes form when $L/2 < \delta h < L$, whereas islands form when $0 < \delta h < L/2$. Under the assumption that the polar PCL is attracted to the substrate (a fact that will be discussed later) and knowing that the film thickness (h) is about 86 ± 8 nm, a two layered structure can be predicted with the formation of islands since $\delta h = 23 \pm 6$ nm $< L/2$. The appearance of featureless (PS) islands when $\delta h < L/2$ on top of patterned perpendicular (PCL) lamellae can again be rationalized using model C as is shown in Fig. 8.

Fig. 9 presents a similar morphology when the sample has been annealed for a longer time (15 h). The height of the islands is more uniform, with a smaller deviation from the mean value, $\delta h = 24 \pm 3$ nm. The film thickness was 113 ± 5 nm. This could correspond to two ABC layers with an additional top-layer formed by islands with $\delta h < L/2$, as expected. An analysis of the domain dimensions shows a wide lamellar thickness distribution. This could be attributed, as in Fig. 4, to an imperfect perpendicular alignment of the lamellae in some regions, probably caused by the opposing forces of microphase separation and

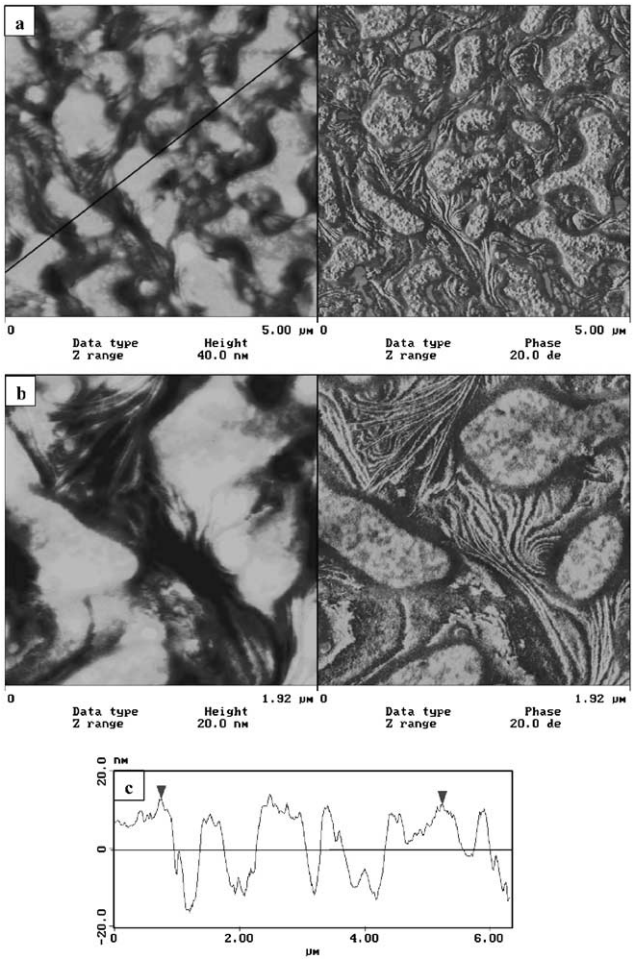

Fig. 9. (a) Topographic (left) and phase (right) AFM images of the surface obtained for $S_{27}B_{15}C_{58}$ spin coated on silicon and annealed at 150 °C for 15 h. (b) Magnification of (a). (c) Cross-sectional line scan.

Fig. 10. Transmission electron micrograph of $S_{35}B_{15}C_{50}$.

crystallization. It should be remembered that this block copolymer is able, under controlled crystallization conditions, to destroy the microphase separated morphology to build spherulites [19,22] In order to investigate whether model C is applicable for block copolymers with a different composition, we investigated the surface morphology of $S_{35}B_{15}C_{50}$. In addition to the samples annealed for 5 and 15 h at 150 °C, we used a shorter annealing time of 1 h. This enabled information about the ordering kinetics of the thin film morphology to be obtained. Before discussing the AFM images, we present the bulk morphology of this block copolymer. Fig. 10 shows that this block copolymer exhibits a lc-morphology. Using OsO_4 as staining agent, the polybutadiene block appears as dark cylinders of diameter D_{PB} between grey polystyrene (L_{PS}) and bright PCL (L_{PCL}) lamellae. A schematic description of this morphology and the corresponding domain dimensions are shown in Fig. 11.

AFM images of $S_{35}B_{15}C_{50}$ annealed for 1 h at 150 °C are shown in Fig. 12(a). A featureless surface is observed with discrete holes randomly located throughout the film. Interestingly, it is possible to observe in Fig. 12(b) as well as in

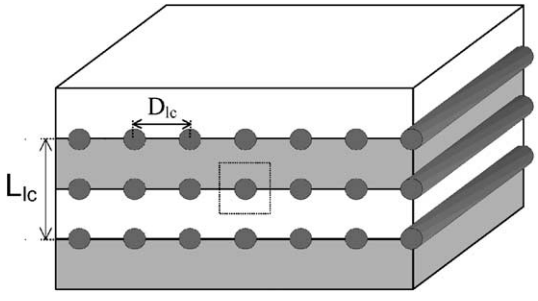

Fig. 11. Schematic description of the lc-morphology. For $S_{35}B_{15}C_{50}$ $L_{lc} = 55 \pm 2$ nm, $L_{PS} = 30 \pm 2$ nm, $D_{PB} = 11 \pm 1$ nm, $D_{lc} = 25 \pm 3$ nm $L_{PCL} = 27 \pm 2$ nm.

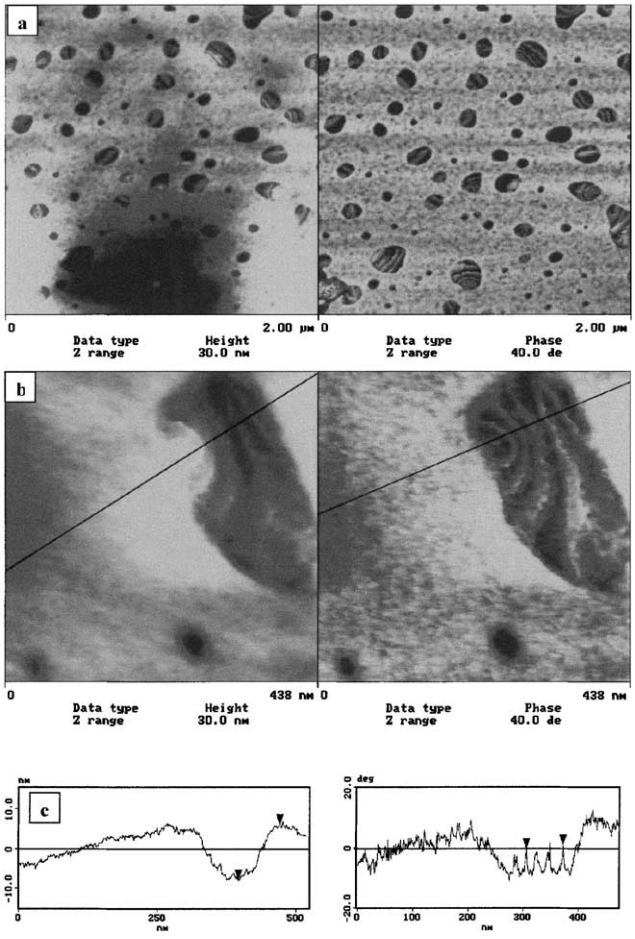

Fig. 12. (a) Topographic (left) and phase (right) AFM images of the surface obtained for $S_{35}B_{15}C_{50}$ spin coated on silicon and annealed at 150 °C for 1 h. (b) Magnification of a hole. (c) Cross-sectional line scans for the topographic and phase images.

detail shown in Fig. 12(c) that the base of the holes reveals a lamellar pattern with a characteristic period of about 22 nm.

To understand this pattern we present, as for the triblock forming a ll-structure, the different ways that such a copolymer could self-assemble on a substrate. A schematic representation is shown in Fig. 13. It is known that PB has a lower surface tension than PS ($\gamma_{PB} = 30$ mN/m, $\gamma_{PS} = 40.7$ mN/m) [29], then it would tend to segregate at the surface. However, if it was on the surface as in model A, it would be detected in the topographic images as higher regions or in the phase images as dark spots [39]. Also, the presence of PB on the surface would mean looping of this block in the surface layer and the coexistence of the PS and PCL blocks in the underlaying layer. For these reasons we discarded model A.

The superficial characteristics shown in Fig. 12 lead us to deduce that the surface of the top and underlying layers are formed by PS (featureless) and PCL (lamellar), respectively. A differentiation of the three components at the bottom of the holes was not possible, as in the $S_{27}B_{15}C_{58}$ sample. The lateral distance could not be correlated with

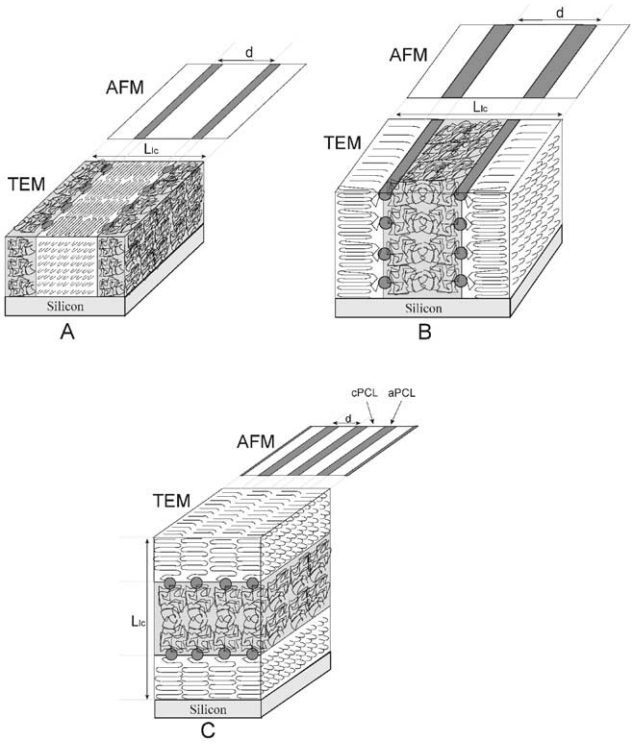

Fig. 13. Schematic representations of the possible ordering of $S_{35}B_{15}C_{50}$ on a substrate.

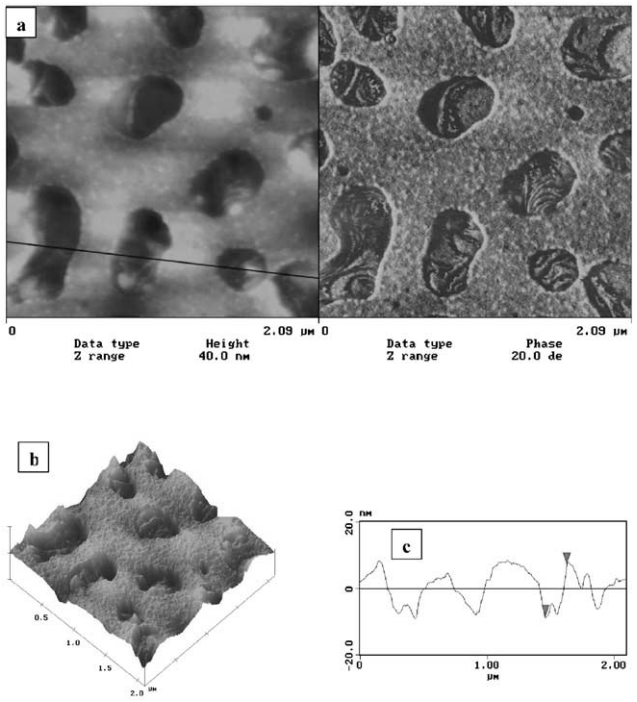

Fig. 14. (a) Topographic (left) and phase (right) AFM images of the surface obtained for $S_{35}B_{15}C_{50}$ spin coated on silicon and annealed at 150 °C for 15 h. Three-dimensional view (b) and cross-sectional line scan (c) of the topographic image.

the bulk long period assuming that the three components were located in the surface of the underlying layer (for example, model B). Therefore, the surface pattern can be explained using model C of Fig. 13. A quantitative evaluation of the depth of the holes using cross-sectional analysis gave a result of about 13 ± 2 nm. Taking into account the bulk long period L_{lc} of 55 nm, there is an apparent contradiction since for $0 < \delta h < L/2$ a pattern with holes is not expected. In order to explain this result, we annealed another sample for a longer time (15 h). AFM images presented in Fig. 14 indicate that the morphology is basically the same, i.e. holes are formed throughout the top layer, in the bottom of which a lamellar pattern can be distinguished. Nevertheless, in contrast to the sample annealed only for 1 h (Fig. 12), the one annealed for 15 h (Fig. 14) shows a mean hole depth of 23 ± 4 nm. This value almost exactly corresponds to $L/2$ and a layer with holes or islands could be expected.

The mean depth of the holes formed through the top layer was 13 ± 2 nm for the sample annealed only for 1 h (Fig. 12). This value agrees very well with half the PS layer. Consequently, we speculate that an annealing time of 1 h was not enough for the chains to completely reptate to the surface and form another ABC layer, and that the PCL blocks of two chains crystallized in an interdigitated fashion, as is depicted schematically in Fig. 15. A similar interdigitation has been previously reported by Reiter et al. [16] for a hydrogenated polybutadiene-*b*-poly(ethylene oxide) diblock copolymer.

In the image of Fig. 12(b) a detailed analysis of a hole could be performed. It is possible to identify a sequence of bright and dark lines corresponding, according to model C, to cPCL and aPCL regions. As mentioned earlier, a characteristic distance of ~22 nm was obtained, very similar to that for $S_{27}B_{15}C_{58}$. This is in agreement with the similar melting points determined from DSC measurements on samples of both copolymers, which were subjected to the same thermal treatments as for the AFM observations (T_m ($S_{27}B_{15}C_{58}$) = 56.5 ± 0.3 °C, T_m ($S_{35}B_{15}C_{50}$) = 55.6 ± 0.3 °C).

The surface tension of cPCL lamellae in the bulk for $S_{27}B_{15}C_{58}$ has been found to be around 6.36 mN/m for the lateral surface and 44.7 mN/m for the fold surface [32]. The latter value is higher than the corresponding one for a PCL homopolymer (106 mN/m) [29]. Comparing these results to the values for PS and PB at room temperature (γ_{PS} = 30 mN/m, γ_{PB} = 40.7 mN/m) [29], it could be predicted that the lateral surfaces of PCL lamellae would be preferentially exposed to air, in contrast to the PCL fold surfaces and PS and PB. In fact, sequences of bright and dark lines corresponding to vertically aligned PCL lamellae were observed on the surfaces of the investigated triblock copolymer films. Nevertheless, when the samples were annealed at high temperature, it was observed that the PS covers the surface partially. This suggests that there are other parameters determining the surface structure. Within these factors, the preferential adsorption of the polar PCL on substrates should be considered when crystallization takes

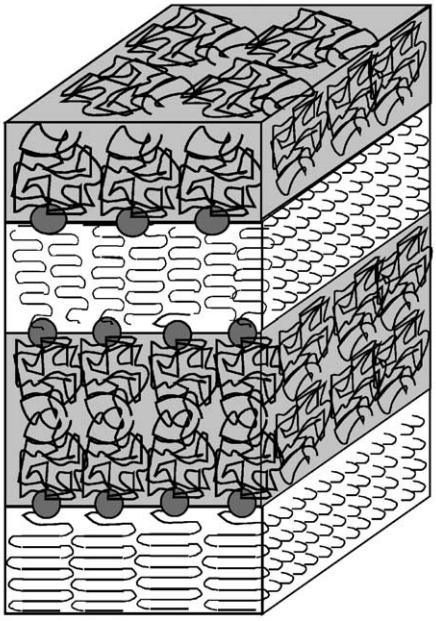

Fig. 15. Schematic drawing of PCL interdigitation.

place after having treated the sample at 150 °C for sufficient time. In the specific case of the silicon substrates, it should be noted that they were used without previous cleaning. Consequently, it is assumed that native SiO_x layers were present. On the other hand, it has been demonstrated that dispersed silica in PCL homopolymer acts as a nucleating agent for this polymer [40]. Therefore, it is reasonable to assume that the PCL block will be preferentially adsorbed on the substrate. With this fact in mind, the presence of PCL or PS on the surfaces will depend, then, on the commensurability between the total film thickness (h) and the long period (L). Taking into account, as mentioned previously, that one layer corresponds to an ABC sequence, asymmetrical (odd) layer numbers will produce a PS surface with holes or islands. Symmetrical (even) layer numbers will produce a PCL surface with holes or islands.

4. Conclusions

The use of AFM led us to demonstrate that spin coated thin films of polystyrene-*b*-polybutadiene-*b*-poly(ε-caprolactone) ABC triblock copolymers are able to build lamellar patterned surfaces. Such patterns are developed from as-cast as well as from samples which were annealed and quenched to room temperature. The coexistence of islands or holes with such lamellar patterns was also observed.

The studied copolymers exhibit ll- and lc-morphologies in the bulk. Based on these morphologies and on the microdomain dimensions obtained from TEM and AFM measurements, we proposed a model for each morphology that could explain the patterned surfaces. By comparing the characteristic lateral distances obtained from AFM and the long period obtained from TEM, we interpret that the lamellae are built by sequences of aPCL and cPCL and that the block copolymer interfaces are parallel to the substrate, reason for why the other components cannot be detected on the surfaces, as shown in models C. The observation of T-shaped grain boundaries between lamellae supports this interpretation. Sharp changes in grain orientation would be prohibited if block copolymer interfaces were perpendicular to the surface as is depicted in models A and B. This interpretation is supported by energetic considerations that indicate that the lateral surfaces of PCL lamellae would be preferentially exposed to air, in contrast to PCL fold surfaces and PS and PB. Nevertheless, the presence of PCL or PS on the surfaces will also depend on the commensurability between the total film thickness (h) and the long period (L). An asymmetrical (odd) layer numbers will produce a PS surface with PCL lamellar patterned holes or islands. A symmetrical (even) layer numbers will produce a PCL lamellar patterned surface with featureless unpatterned holes or islands. All these facts could be rationalized by using model C.

How the surfaces can change varying the crystallization conditions is now under research and will be subject of future works.

Acknowledgements

V. Balsamo acknowledges the support from CONICIT through grant S1-96001934. S. Collins was supported by EPSRC grant GR/N00678 to IWH. We thank Dr Neil Thomson, Department of Physics and Astronomy, University of Leeds, for help with contact mode AFM and TSU Gustavo Gil and Lic. Edgar Cañizales, Laboratorio de Polímeros, Universidad Simón Bolívar, for the TEM images.

References

[1] Rangarajan P, Register RA, Fetters LJ. Macromolecules 1993;26:4640.
[2] Rangarajan P, Register RA, Adamson DH, Fetters LJ, Bras W, Naylor S, Ryan AJ. Macromolecules 1995;28:4932.
[3] Ryan AJ, Fairclough JPA, Hamley IW, Mai SM, Booth C. Macromolecules 1997;30:1723.
[4] Mai SM, Fairclough JPA, Viras K, Gorry PA, Hamley IW, Ryan AJ, Booth C. Macromolecules 1997;30:8392.
[5] Hamley IW, Fairclough JPA, Bates FS, Ryan AJ. Polymer 1998;39:1429.
[6] Douzinas KC, Cohen RE. Macromolecules 1992;25:5030.
[7] Ryan AJ, Hamley IW, Bras W, Bates FS. Macromolecules 1995;28:3860.
[8] Quiram DJ, Register RA, Marchand GR. Macromolecules 1997;30:4551.
[9] Cohen RE, Bellare A, Drzewinski MA. Macromolecules 1994;24:2321.
[10] Hamley IW, Fairclough JPA, Terrill NJ, Ryan AJ, Lipic PM, Bates FS, Towns-Andrews E. Macromolecules 1996;29:8835.

[11] Hamley IW, Fairclough JPA, Ryan AJ, Bates FS, Towns-Andrews E. Polymer 1996;37:4425.
[12] Quiram DJ, Register RA, Marchand GR, Adamson DH. Macromolecules 1998;31:4891.
[13] Loo YL, Register RA, Ryan AJ. Phys Rev Lett 2000;84:4120.
[14] Hamley IW. Adv Polym Sci 1999;148:113.
[15] Reiter G, Castelein G, Hoerner P, Riess G, Blumen A, Sommer JU. Phys Rev Lett 1999;83:3844.
[16] Reiter G, Castelein G, Hoerner P, Riess G, Sommer JU, Floudas G. Eur Phys J E 2000;2:319.
[17] Hamley IW, Wallwork ML, Smith DA, Fairclough JPA, Ryan AJ, Mai SM, Yang YW, Booth C. Polymer 1998;39:3321.
[18] Fairclough JPA, Mai SM, Matsen MW, Bras W, Messe L, Turner S, Gleeson A, Booth C, Hamley IW, Ryan AJ. J Chem Phys 2001;114:5425.
[19] Balsamo V, von Gyldenfeldt F, Stadler R. Macromol Chem Phys 1996;197:3317.
[20] Balsamo V, Stadler R. Macromol Symp 1997;117:153.
[21] Balsamo V, Müller AJ, von Gyldenfeldt F, Stadler R. Macromol Chem Phys 1998;199:1063.
[22] Balsamo V, Stadler R. Macromolecules 1999;32:3994.
[23] Kim G, Jackson CL, Balsamo V, Libera M, Stadler R, Han CC. SPE ANTEC Proc 1999;II:1734.
[24] Kim G, Han CC, Libera M, Jackson CL. Macromolecules 2001;34:7336.
[25] Pickett GT, Balazs AC. Macromol Theor Simul 1998;7:249.
[26] Elbs H, Fukunaga K, Stadler R, Sauer G, Magerle R, Krausch G. Macromolecules 1999;32:1204.
[27] Fukunaga K, Elbs H, Magerle R, Krausch G. Macromolecules 2000;33:947.
[28] Balsamo V, von Gyldenfeldt F, Stadler R. Macromol Chem Phys 1996;197:1159.
[29] Mark JE, editor. Physical properties of polymers handbook. New York: AIP Press, 1996.
[30] Gido SP, Thomas EL. Macromolecules 1999;27:6137.
[31] Wunderlich B. Macromolecular physics: crystal melting, vol. 3. New York: Academic Press, 1980.
[32] Müller AJ, Balsamo V, Carrizales P, Gil G. Submitted for publication.
[33] Balsamo V, Gil G, Urbina de Navarro C, Hamley IW, von Gyldenfeldt F, Abetz V, Cañizales E. Submitted for publication.
[34] Limary R, Green PF. Macromolecules 1999;32:8167.
[35] Coulon G, Russell TP, Deline VR, Green PF. Macromolecules 1989;22:5677.
[36] Collin B, Chatenay D, Coulon G, Ausserre D, Gallot Y. Macromolecules 1992;25:1621.
[37] de Jeu WH, Lambooy P, Hamley IW, Vaknin D, Pedersen JS, Kjaer K, Seyger R, van Hutten P, Hadziioannou G. J Phys II, Fr 1993;3:139.
[38] Orso KA, Green PF. Macromolecules 1999;32:1087.
[39] Stocker W, Beckmann J, Stadler R, Rabe JP. Macromolecules 1996;29:7502.
[40] Balsamo V, Müller AJ, Sánchez A, Aguilera E. In preparation.